Separation and Purification Technology 204 (2018) 336–344

Contents lists available at ScienceDirect

Separation and Purification Technology

journal homepage: www.elsevier.com/locate/seppur

Effect of polyacid dopants on the performance of polyaniline membranes in organic solvent nanofiltration

Junjie Shen[a,b], Salman Shahid[a,b], Adem Sarihan[a,b,c], Darrell A. Patterson[a,b], Emma A.C. Emanuelsson[b,*]

[a] Centre for Advanced Separations Engineering, University of Bath, Bath BA2 7AY, United Kingdom
[b] Department of Chemical Engineering, University of Bath, Bath BA2 7AY, United Kingdom
[c] Higher Vocational School, Bilecik Seyh Edebali University, Bilecik 11210, Turkey

ARTICLE INFO

Keywords:
Polyaniline
Organic solvent nanofiltration
Polyacid
Dopant
Molecular weight cut-off

ABSTRACT

Polyaniline (PANI) has been widely explored as a promising membrane material, but the trade-off between porosity and stability limits its widespread application in organic solvent nanofiltration (OSN). Here we present a simple approach to prepare PANI membranes with excellent chemical stability and rejection performance in OSN by employing polyacids as PANI dopants for the first time. The PANI membranes were doped with two polyacids with different molecular weights (MW) and acid dissociation constants (pKa): namely poly(4-styrenesulfonic acid) (PSSA, MW: 75000 g mol^{-1}, pKa: 0.94) and poly(2-acrylamido-2-methyl-1-propanesulfonic acid) (PAMPSA, MW: 800000 g mol^{-1}, pKa: 0.87), and were compared with a small acid (HCl) doped PANI membrane. The polyacid doped membranes, PANI-PSSA and PANI-PAMPSA, obtained dense structures with increased hydrophilicity due to strong intermolecular interactions between the PANI and the polyacids. Stability tests showed that the PANI-PSSA and PANI-PAMPSA were stable in a wide range of polar and nonpolar solvents, while the undoped PANI and PANI-HCl had poor stability in these solvents. The swelling degree and permeance of the doped membranes decreased with the increase of the dopant MW. The PANI-PAMPSA membrane exhibited a molecular weight cut-off (MWCO) in the nanofiltration (NF) range of 400 g mol^{-1} in methanol and isopropanol, while the PANI-HCl and PANI-PSSA membranes were in the ultrafiltration (UF) range. This study demonstrates that polyacid doping can make stable and nanoporous PANI membranes for OSN applications without the need for crosslinking. This simple approach can be used to design new classes of OSN membranes for challenging separation processes in the future.

1. Introduction

Organic solvent nanofiltration (OSN), also known as solvent resistant nanofiltration (SRNF), has gained momentum in recent years with applications such as solvent exchange, catalyst recovery and recycling, in the bio-technology, the chemical and the pharmaceutical industries [1,2]. OSN separates molecules (below 1000 g mol^{-1}) based on three major mechanisms: size exclusion (sieving), charge interaction (Donnan effect), and solute-membrane affinity (*e.g.*, hydrophobic attraction, hydrogen bonding) [3–5]. OSN generates less waste streams and only requires moderate energy consumption [6,7], in comparison to conventional separation techniques, like distillation, extraction, crystallization and preparative chromatography, potentially achieving a reduction of energy consumption by 90% [8]. OSN membranes are nearly exclusively polymeric and ceramic. Ceramic membranes are more robust due to their higher chemical and thermal resistance, and they do not show any compaction under pressure and are easy to clean. They are however, more expensive, brittle and are difficult to be prepared for the molecular weight cut-off (MWCO) range lower than 450 g mol^{-1} [1,2]. On the contrary, advantages of polymeric membranes are much lower MWCO ranges and more compact modules which are essential for large scale OSN applications [1]. The main current challenge for polymeric membranes is the development of materials that have high chemical and thermal resistance and long-term stability in a wide range of organic solvents [9,10].

Polyaniline (PANI) has been extensively studied as a material for membrane fabrication due to its easy synthesis, good environmental stability, and most importantly, the unique doping/dedoping properties [11–26]. PANI has a π-conjugated structure which consists of alternating single bonds (amines) and double bonds (imines) along the backbone. The oxidation states of PANI range from fully reduced (leucoemeraldine) to fully oxidized (pernigraniline). The intermediate

* Corresponding author.
E-mail address: E.A.Emanuelsson-Patterson@bath.ac.uk (E.A.C. Emanuelsson).

https://doi.org/10.1016/j.seppur.2018.04.034
Received 23 January 2018; Received in revised form 27 March 2018; Accepted 14 April 2018
Available online 16 April 2018
1383-5866/

oxidation state (emeraldine), which has a structure with equal proportions of amines and imines, is the only form capable of carrying charge [11]. The emeraldine base (EB) becomes the electrically conducting emeraldine salt (ES) upon protonation [11]. The EB form of PANI can be doped by acid and de-doped by exposure to a base [27,28].

Anderson et al. found that the as-cast PANI membrane could obtain gas permeation properties via the doping/dedoping cycle using halogen acids (HF, HCl, HBr, and HI) and ammonium hydroxide (NH_4OH) [13]. The doping process forced the membrane polymer network to reorganize conformationally, in order to accommodate the proton and the counterion of the acid. The subsequent dedoping process removed the acid and induced porosity in the membrane matrix [13]. The novel concept of using acid dopants to create porosity in PANI membranes was extended to OSN applications by Loh et al. [29]. They doped PANI membranes with various low molecular weight (MW) organic acids (in the MW range of 100–400 g mol^{-1}) by direct addition of the acids into the casting solutions before membrane fabrication [29]. After removing the acids by alkaline extraction, the PANI membranes were treated by either thermal [30] or chemical [29] crosslinking to achieve good solvent stability. However, the crosslinking process irreversibly decreased the free volume of the membrane to an extent that even small molecules could not pass and therefore cancelled any differences caused by different acid dopants [30]. To date, the trade-off between porosity and stability still remains a challenge for preparing OSN membranes using PANI.

This study presents a new strategy to fabricate PANI membranes by using polyacids as the acid dopants. Polyacids have larger MW and higher conformational flexibility in comparison to inorganic and small organic acids [31,32]. Previous studies have found that small acids, such as HCl, form a single-strand structure with PANI, while polyacids form a double-strand structure with PANI because the polyacids can easily adapt their conformation to match the structure of PANI [33,34]. The double-strand structure induces strong intermolecular interactions (e.g., hydrogen bonding, π-interactions, and electrostatic interactions), which confer oxidative stability into PANI [35]. Considering that acid doping occurs on the same site as crosslinking [29], we hypothesized that high porosity and stability of PANI could be obtained by polyacid doping without the need for crosslinking, thus overcoming the current trade-off dilemma of PANI membranes.

Two polyacids, poly(4-styrenesulfonic acid) (PSSA) and poly(2-acrylamido-2-methyl-1-propanesulfonic acid) (PAMPSA) will be investigated and compared with HCl in this study. PSSA and PAMPSA are flexible-backbone polyacids with regular distribution of sulfonic groups along the macromolecules, which should allow them to easily form interpolymer complexes with other polymers [34]. These three dopants had different MW, acidity, and hydrophilicity to further evaluate how these parameters influence the properties of the membrane. The physical, chemical and separation properties of the doped membranes will be analyzed by a variety of characterization methods (such as Fourier transform infrared spectroscopy (FT-IR), X-ray photoelectron spectroscopy (XPS), scanning electron microscopy (SEM), and contact angle measurement) and lab-scale nanofiltration experiments. The effect of dopant on membrane performance will be investigated by determining a relationship between the three dopants, the solvent (a range of polar and non-polar solvents) and the membrane swelling behavior and will be related to membrane separation parameters such as membrane permeance and MWCO.

2. Experimental

2.1. Chemicals

Analytical grade aniline, ammonium persulfate (APS), HCl, PSSA, N-methyl-2-pyrrolidone (NMP), 4-methyl piperidine (4MP), poly(propylene) glycol (PPG, MW = 725 g mol^{-1}) were obtained from Sigma-Aldrich, UK. PAMPSA and HPLC grade toluene, acetone, isopropanol, ethanol and methanol were supplied by Fisher Scientific, UK. Tripropylene glycol (MW = 192 g mol^{-1}), PPG (MW = 400 g mol^{-1}) and PPG (MW = 1000 g mol^{-1}) were purchased from Alfa Aesar, UK. The non-woven polyethylene/polypropylene mixture backing layer (Novatexx 2431, 140 μm) was supplied by Freudenberg Filter, Germany. Deionized (DI) water was produced by an ELGA deionizer from PURELAB Option, USA.

Table 1
MW and pKa values of different acid dopants.

Dopant	MW (g mol^{-1})	pKa
HCl	36.46	−6.30 [36]
PSSA	75,000	0.94
PAMPSA	800,000	0.87

The MW and the acid dissociation constant (pKa) values of HCl, PSSA and PAMPSA are summarized in Table 1. The pKa values of PSSA and PAMPSA were calculated from the titration curves by 1 M NaOH (See Supporting Information Fig. S1). PSSA and PAMPSA had higher pKa than HCl, which means they were weaker than HCl at donating protons. Thus it could be expected that the doping degrees of the PANI-PSSA and PANI-PAMPSA membranes should be lower than that of the PANI-HCl membrane.

2.2. Synthesis of PANI powder

PANI powder was synthesized by oxidative polymerization of aniline. 0.2 mol of aniline and 0.2 mol of APS were dissolved in 1 M HCl, separately. The APS solution was slowly added into the aniline solution by a peristaltic pump at a speed of 20 mL h^{-1}. The temperature was controlled at 15 °C, and the mixture was left for 24 h for full polymerization. The obtained PANI powder was in the protonated state (PANI-ES). It has been generally observed that PANI-ES is unable to dissolve in most organic solvents [37]. In order to increase its processability for membrane fabrication, the PANI-ES powder was deprotonated with 33.3% (w/v) ammonia solution to become PANI-EB. The PANI-EB powder was then washed with DI water and methanol, and dried in a vacuum oven at 60 °C for 24 h. The dry PANI-EB powder was ground in a mortar to obtain a fine product.

2.3. Fabrication and doping of PANI membranes

PANI membranes were prepared by the immersion precipitation method [38], where NMP dissolved the PANI-EB powder and 4MP acted as the gelation inhibitor [39]. Firstly, 4MP was added to NMP and stirred about 5 min; secondly, appropriate amount of PANI-EB powder was added into the mixture of NMP and 4MP to make a 20% (w/w) solution; finally, the solution was stirred at 300 rpm for 4 h to obtain a homogeneous mixture, and left to stand for 4 h for degassing. The solution was then cast on the non-woven backing layer to make a 200 μm thick film using an adjustable casting knife (4340 Automatic Film Applicator, Elcometer, UK). The film was fully immersed into a coagulation bath containing DI water. Due to the solvent and non-solvent exchange, PANI precipitation occurred and a solid polymeric membrane was formed.

In the doping process, three acid dopants were used, including one inorganic acid (HCl) and two polyacids (PSSA and PAMPSA). The doping solutions were 1 M HCl solution, 10% (w/w) PSSA solution, and 10% (w/w) PAMPSA solution. The PANI membranes were initially rinsed with DI water, and then soaked in the certain doping solution. The HCl solution was left in a jar at room temperature for 3 h. To facilitate the doping process of polyacid, the PSSA and PAMPSA solutions were sealed and heated in an oven at 80 °C for 3 h. The doped membranes were rinsed with DI water and dried in air. A color change from dark blue to dark green was observed in the doped membranes,

implying the completion of the doping process.

2.4. Membrane characterization

The chemical compositions of the undoped and doped PANI membranes were determined using a FT-IR spectrometer (Spectrum 100, PerkinElmer, USA) fitted with an attenuated total reflectance (ATR) accessory. Each FT-IR spectrum had 32 scans with 4 cm^{-1} resolution. XPS spectra were obtained on a spectrophotometer (K-Alpha, Thermo Scientific, UK) utilizing a monochromatic Al-Ka X-ray source (energy = 1486.6 eV). XPS spectra were calibrated to the C 1 s hydrocarbon peak at 284.6 eV. Peak fitting was carried out by the CasaXPS software (version 2.3.16) using a Shirley background. The electrical resistivity of each membrane was measured using a four-point multi-height probe (RM3000, Jandel Engineering Limited, UK) at room temperature. The electrical conductivity was calculated as the reciprocal of electrical resistivity. The morphological properties of the membranes were investigated by a SEM (JSM-6480LV, JEOL, Japan). SEM images on both the surface and the cross-section were captured for each membrane and a representative cross-section was obtained by fracturing the membrane in liquid nitrogen. The samples were mounted onto SEM stubs and coated with gold using a sputter coater (S150B, Edwards, USA). The accelerating voltage was 10 kV. The hydrophilicities of the membranes were measured by the sessile drop method using a contact angle instrument (OCA 15Pro, Dataphysics, Germany).

2.5. Swelling and stability tests

Methanol, ethanol, isopropanol, acetone, and toluene were chosen as the organic solvents to determine the membrane swelling and stability. In terms of the polarity, methanol, ethanol and isopropanol are polar protic solvents, acetone is a polar aprotic solvent, and toluene is a nonpolar solvent [40]. The potential swelling capabilities of these solvents were quantified by using the Hansen solubility parameters. Hansen solubility parameters measure the extent of the dispersive, polar, and hydrogen bonding interactions between the solvent and the polymer [41]. Technically, the polymer will not mix with the bulk solvent but rather absorb the solvent into its structure, increasing in both size and mass. As a general rule, solvents and polymers that exhibit similar Hansen solubility parameters are expected to interact strongly with each other and cause significant polymer swelling [42]. The Hansen solubility parameters (25 °C) for the solvents are as follow: 29.6 $MPa^{0.5}$ (methanol), 26.5 $MPa^{0.5}$ (ethanol), 23.6 $MPa^{0.5}$ (isopropanol), 19.9 $MPa^{0.5}$ (acetone), 18.2 $MPa^{0.5}$ (toluene) [41]. The Hansen solubility parameter (25 °C) for the undoped PANI is 22.2 $MPa^{0.5}$ [43].

The undoped and doped PANI membranes were cut into small samples (2cm × 2 cm) and dried in the vacuum oven. The dried membrane samples (of known mass) were allowed to equilibrate with excess of the solvent in a sealed flask at 25 °C for 1 h. The swollen membranes were taken from the solvent and quickly dried with a filter paper to remove solvent from the external surface. The mass of the swollen membranes was then determined. The mass swelling degree (Q_m) was calculated using equation (1):

$$Q_m = (m_{wet} - m_{dry})/m_{dry} \quad (1)$$

where m_{wet} is the mass of the swollen membrane after equilibrium and m_{dry} is the mass of the dry membrane.

The stability of the PANI membranes in the solvents were determined by immersing the membrane sample in the solvent for one week (same conditions as per swelling test). After one week, the swollen membrane samples were taken from the solvent and dried in the vacuum oven. The mass change of the dry membrane before and after soaking in the solvent indicates whether the membrane dissolves in the certain solvent. The swelling and stability test was repeated three times for each membrane.

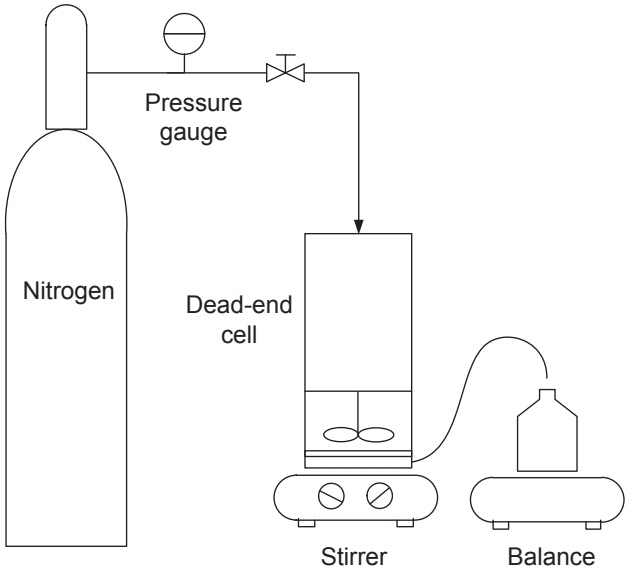

Fig. 1. Schematic of the dead-end pressure filtration system.

2.6. Nanofiltration setup and MWCO determination

Nanofiltration experiments were conducted in dead-end mode using a stainless-steel pressure filtration cell (HP4750, Sterlitech Corporation, USA). The schematic of the experimental set-up is illustrated in Fig. 1. The membrane was placed on the base of the cell with an effective area of 14.6 cm^2. During filtration, the cell was immersed in a water bath at 25 °C, pressurized with nitrogen at 30 bar, and stirred by a magnetic stirrer at 300 rpm. The permeate flow was measured using an electronic balance (EK-300i, A&D Weighing, USA). Each membrane was preconditioned with pure solvent until a stable flux was achieved. The permeance (P) was determined using equation (2):

$$P = Q_P/(A \times p) \quad (2)$$

where Q_P is the permeate flow at provided test conditions, p is the applied pressure and A is the membrane active area.

MWCO is defined as the lowest MW at which 90% of a solute is retained by the membrane [44]. This value was obtained by plotting the rejection of solutes versus their MW, and interpolating this curve to find the MW corresponding to 90% rejection. The MWCO determination method used in this study was described in detail elsewhere [45]. Briefly, the mixture solution to determine the MWCO contained 4 g L^{-1} of tripropylene glycol (MW = 192 g mol^{-1}), PPG (MW = 400 g mol^{-1}), PPG (MW = 725 g mol^{-1}) and PPG (MW = 1000 g mol^{-1}) in a certain type of solvent. The reason to choose these MWs was to cover the typical MWCO range for nanofiltration (NF) which is 200–1000 g mol^{-1} [46]. For each experiment, 40 mL of feed solution was added into the cell and 20 mL of permeate solution was collected. The concentrations of PPG oligomers in the feed, permeate and retentate solutions were determined by a HPLC equipped with a reverse-phase C18 column and an evaporative light scattering detector (ELSD) (1260 Infinity, Agilent Technologies, USA). Calibration curves were constructed by measuring a series of mixture solutions of PPG oligomers with concentration ranging from 0.2 to 8 g L^{-1}. The calibration curves in isopropanol can be found in Fig. S2, while the calibration curves in methanol and acetone were included elsewhere [45].

The rejection (R) of each oligomer was calculated using equation (3):

$$R = (1 - C_P/C_R) \times 100\% \quad (3)$$

where C_P and C_R are the permeate concentration and the retentate concentration, respectively. The MWCO values of the PANI membranes were determined by plotting the rejections of all the oligomers against

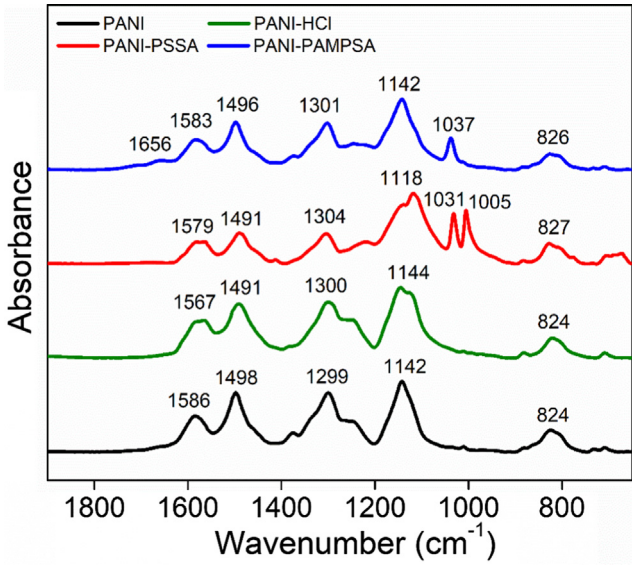

Fig. 2. FT-IR spectra of PANI, PANI-HCl, PANI-PSSA, and PANI-PAMPSA membranes.

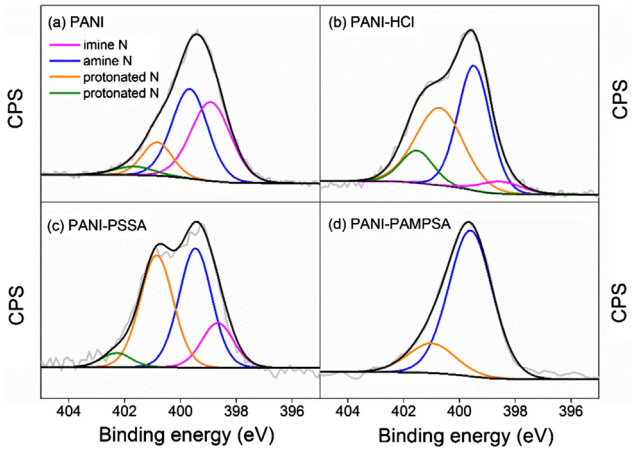

Fig. 3. N 1s core-level spectra of (a) PANI, (b) PANI-HCl, (c) PANI-PSSA and (d) PANI-PAMPSA membranes.

their MWs.

3. Results and discussion

3.1. Characterization of the PANI membranes

FT-IR. Fig. 2 shows the FT-IR spectra of the PANI, PANI-HCl, PANI-PSSA, and PANI-PAMPSA membranes. Typical absorption bands of the undoped PANI were observed at 1586 cm^{-1} (quinoid C═C stretching), 1498 cm^{-1} (benzenoid C═C stretching), 1299 cm^{-1} (aromatic amine C—N stretching), 1142 cm^{-1} (aromatic imine C═N stretching) and 824 cm^{-1} (C—C bending) [22,47,48]. For the doped PANI membranes, the presence of absorption bands from the dopants confirmed their successful incorporation into PANI structures. Specifically, the characteristic bands of O═S═O stretching of PSSA were observed at 1031 cm^{-1} and 1005 cm^{-1} in PANI-PSSA [34]. The bands of O═S═O stretching and C═O stretching of PAMPSA were observed at 1037 cm^{-1} and 1656 cm^{-1} in PANI-PAMPSA [34].

In the doping process, the counterions from the acid dopants, namely the chloride from HCl and the sulfonic groups from PSSA and PAMPSA, provide the necessary protons to the polymer backbone of PANI [49]. It is well established that the molecular incorporation of PSSA and PAMPSA in PANI matrix is through the interaction between sulfonic groups of the polyacids and nitrogen atoms of PANI [34]. As shown in Fig. 2, in the doped PANI membranes the bands of quinoid and benzenoid stretching were shifted to a lower wavelength due to the doping effect [34,50,51]. The doping effect was less pronounced in the PANI-PAMPSA as the band shift was shorter. A possible explanation is that the large MW of PAMPSA constrained its diffusion in the PANI matrix, thereby resulting in a lower doping level compared to the small MW dopants [52,53].

XPS. The intrinsic oxidation state and protonation level of the PANI membranes were monitored through the N 1s core-level spectra (Fig. 3). Three nitrogen species were differentiated in the properly curve-fitted spectra, namely the imine (═N—) at 398.5 eV, the amine (—NH—) at 399.5 eV, and the protonated nitrogen (N^+) located above 400 eV [28,54,55]. The ratio of nitrogen species to total nitrogen content, the doping level (the percent of protonated nitrogen to the total nitrogen content), and the electrical conductivity are given in Table 2.

The undoped PANI had approximately equal amounts of imine and amine species, which was consistent with the intrinsic redox state of the EB form of PANI (Fig. 3(a)). The small ratio of protonated nitrogen (0.17) was probably associated with surface oxidation products, interchain hydrogen bonding, and contribution of the imine satellite [28]. In the N 1s core-level spectrum of PANI-HCl (Fig. 3(b)), the ratio of the imine nitrogen decreased significantly to only 0.05 and the ratio of the protonated nitrogen increased to 0.52, corresponding to a doping level of 52%. This agrees with the general belief that protonation occurs predominantly at the imine nitrogen atoms [28]. The N 1s core-level spectrum of PANI-PSSA was similar to that of PANI-HCl but with a lower doping level of 43% (Fig. 3(c)). This is because PSSA is less capable to donate protons than HCl (Table 1). A positive correlation between the doping level and electrical conductivity was observed among the undoped PANI, PANI-PSSA, and PANI-HCl (Table 2). Through acid doping, the imine sites were protonated to the bipolaronic form, which was responsible for the increased conductivity [56,57].

Table 2
XPS and conductivity results of the undoped and doped PANI membranes.

Membrane	Imine N	Amine N	Protonated N	Doping level (%)	Conductivity (S cm^{-1})
PANI	0.41	0.42	0.17	17	6.5×10^{-7}
PANI-HCl	0.05	0.43	0.52	52	2.7×10^{-2}
PANI-PSSA	0.07	0.50	0.43	43	2.4×10^{-4}
PANI-PAMPSA	0	0.82	0.18	NA	1.3×10^{-4}

It is noteworthy that only the amine and the protonated nitrogen species appeared in the spectrum of PANI-PAMPSA (Fig. 3(d)). This was because the residual PAMPSA macromolecules covered the surface of PANI-PAMPSA and consequently, the amine nitrogen from PAMPSA shielded nitrogen signals from PANI-PAMPSA. Thus, the doping level of PANI-PAMPSA could not be quantitatively determined through the N 1s core-level spectra. Nevertheless, given the FT-IR, pKa and conductivity results, the actual doping level of PANI-PAMPSA was expected to be lower than that of PANI-PSSA.

SEM images of the membrane surfaces are shown in Fig. 4. The PANI and PANI-HCl membranes had irregular bulges on the surface, which was due to the heterogeneous accumulation of PANI granules. Oppositely the PANI-PSSA and PANI-PAMPSA membranes had much smoother skin layers, which was attributed to the homogenous coverage of PSSA and PAMPSA macromolecules on the membrane. No pinhole or pore structures were seen at the magnification used (5000x). The cross-sectional images (Fig. 5) reveal that the undoped and doped PANI membranes all had an integrally skinned asymmetric structure, where a thin, dense skin layer was at the top of a porous support layer. Solution rejection and hydraulic resistance occurred mostly across the thin layer. The bulk support layer was dominantly spongy interspersed with many finger-like macrovoids. The formation of macrovoids in such

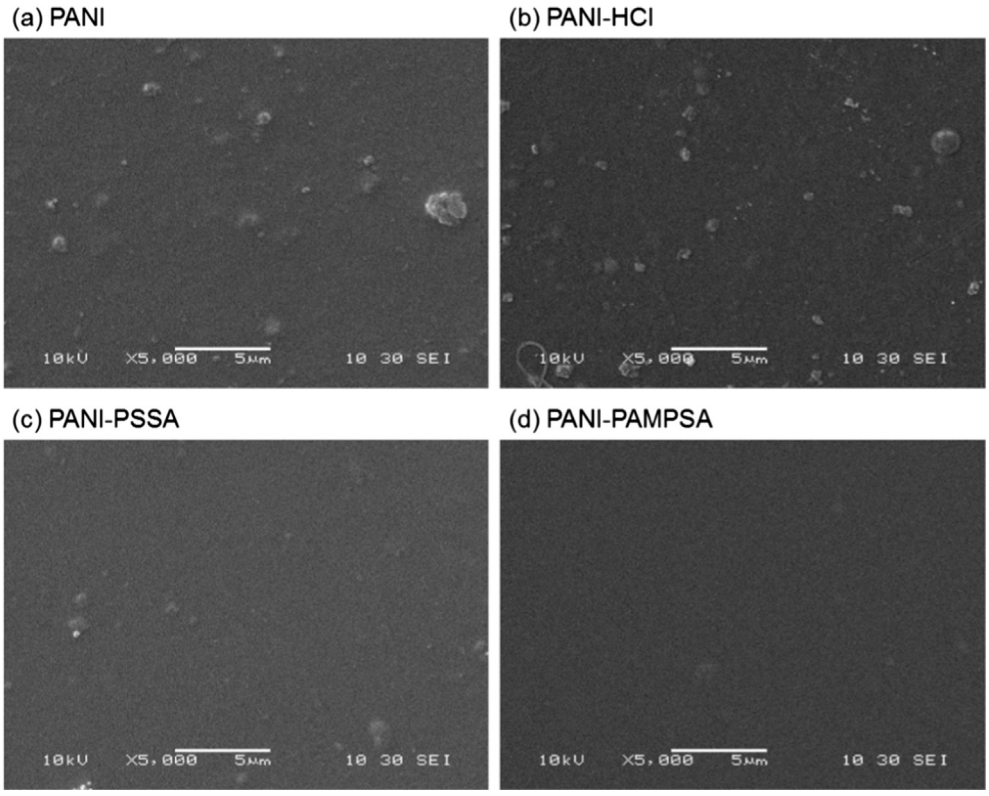

Fig. 4. SEM images of the surface of (a) PANI, (b) PANI-HCl, (c) PANI-PSSA and (d) PANI-PAMPSA membranes.

phase-inversion membranes was due to the instantaneous onset of liquid–liquid demixing [29,58]. These macrovoids might result in membrane compaction during filtration. The cross-sectional images of the different PANI membranes were highly similar, which suggested that the acid doping under the conditions used did not affect the porous support structure in the asymmetric membrane layers.

Hydrophilicity of the PANI membrane was estimated by measuring the apparent contact angle of the membrane surface. A hydrophilic

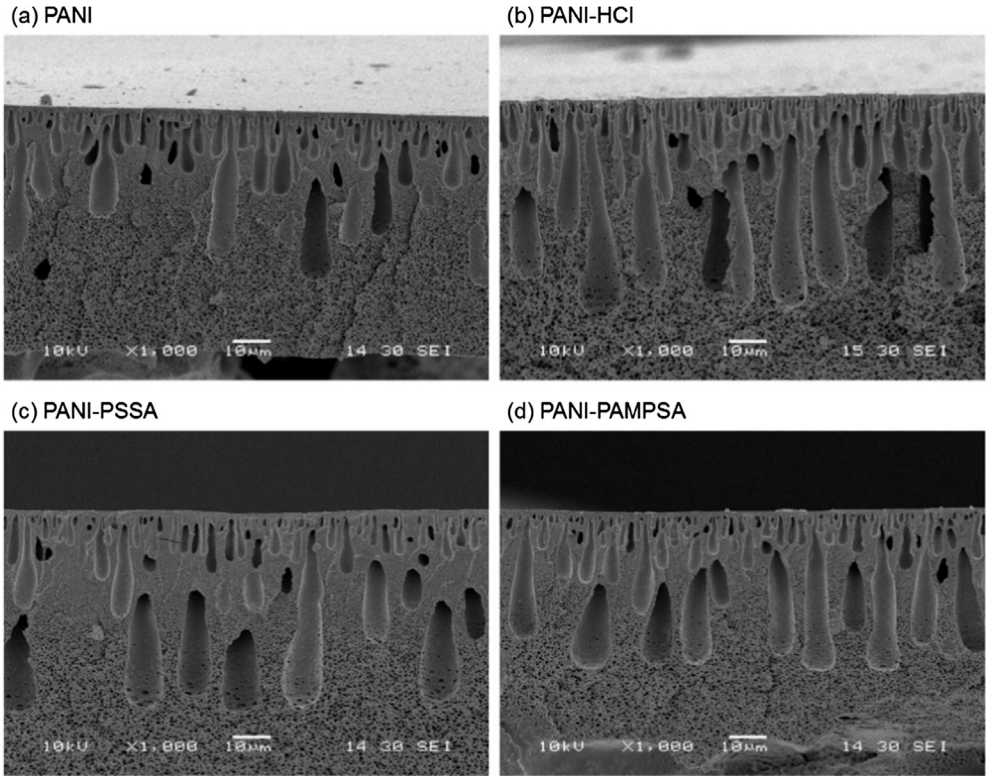

Fig. 5. SEM images of the cross-section of: (a) PANI, (b) PANI-HCl, (c) PANI-PSSA and (d) PANI-PAMPSA membranes.

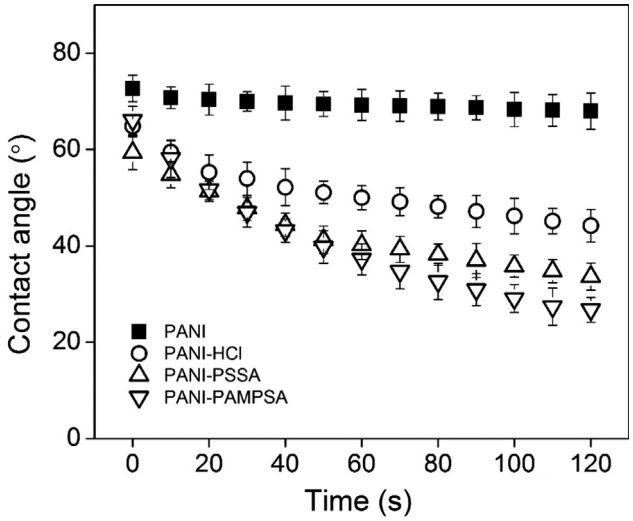

Fig. 6. The apparent contact angle of PANI, PANI-HCl, PANI-PSSA, and PANI-PAMPSA membranes over time.

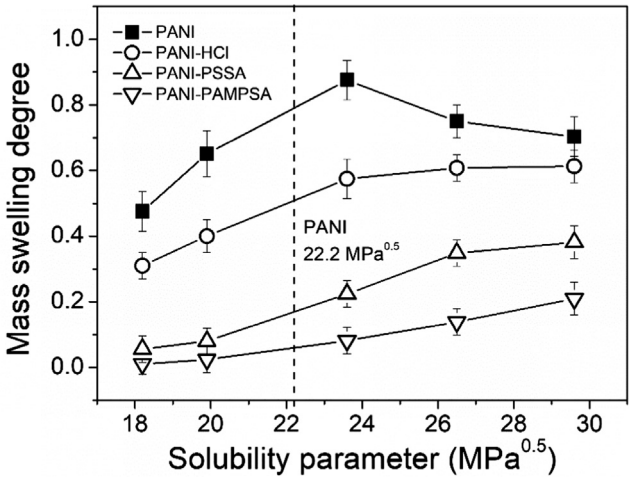

Fig. 7. Mass swelling degree of PANI membranes in different solvents as a function of the Hansen solubility parameter.

membrane has high affinity to water, which results in a contact angle less than 90°. As seen from Fig. 6, all the four PANI membranes were hydrophilic. The contact angle of the membranes decreased in the order of PANI > PANI-HCl > PANI-PSSA > PANI-PAMPSA. Therefore, the hydrophilicity followed the opposite order: PANI < PANI-HCl < PANI-PSSA < PANI-PAMPSA. Previous work reported that the doping treatment significantly improved the hydrophilicity of the PANI membranes [59]. The hydrophilicity of PANI-HCl, PANI-PSSA and PANI-PAMPSA arose from the hydrophilic functional groups from the corresponding dopants, *i.e.*, chloride from HCl, sulfonic group from PSSA, and sulfonic, carbonyl and amide groups from PAMPSA. Between the two sulfonic dopants, PSSA is less hydrophilic than PAMPSA due to the presence of the hydrophobic phenylene groups [60]. Therefore, PANI-PSSA was less hydrophilic than PANI-PAMPSA. Additionally, residual dopants existed on the membrane surface even though the membrane was gently rinsed with DI water. These dopants produced dissociative ions that distributed randomly in the membrane, which again facilitated the interaction between the membrane and water [61].

3.2. Membrane swelling and stability

Determining the extent of swelling in the membranes is a key step to fully understand their behavior, as when swollen the separation properties are different to those in their non-swollen state [62,63]. Fig. 7 shows the mass swelling degrees of PANI membranes as a function of the Hansen solubility parameters. The mass swelling degree of the undoped PANI increased from 0.47 to 0.87 as the Hansen solubility parameter increased from 18.2 to 23.6 MPa$^{0.5}$, and then reduced at the higher end of solubility parameter. The maximum swelling occurring at 23.6 MPa$^{0.5}$ corresponded favorably to the Hansen solubility parameter of 22.2 MPa$^{0.5}$ for PANI. Solvents close to this value were likely to swell the polymer most, and solvents far from this value had negligible effect on swelling. The similar curved trend was reported for the swelling of polydimethylsiloxane (PDMS) membrane in the solubility parameter range 14.3–29.2 MPa$^{0.5}$, where a maximum expansion was attained at 15.5 MPa$^{0.5}$ which was the solubility parameter for PDMS [62].

However, the swelling trend of the doped PANI membranes was different, which did not decrease at Hansen solubility parameter greater than 23.6 MPa$^{0.5}$. On the contrary, the swelling degrees of PANI-PSSA and PANI-PAMPSA continued to increase at higher solubility parameter values. As discussed in Section 3.1, acid dopant significantly increased the hydrophilicity of PANI. This means that the doped PANI membrane, as an integral, had a higher solubility parameter than the undoped PANI. An increase in the solubility parameter of PANI resulted in a shift of the maximum swelling towards the higher end of solubility parameter. In consequence, the swelling degree of the doped PANI continued to grow with increasing solubility parameter, especially in the case of PANI-PSSA and PANI-PAMPSA which obtained higher degrees of hydrophilicity after doping.

Fig. 7 also shows that the acid dopants with larger MW resulted in a smaller swelling degree. Specifically, the swelling degree of PANI membranes in the same solvent decreased in the sequence: PANI > PANI-HCl > PANI-PSSA > PANI-PAMPSA. This can be explained by a decrease in the free volume of the membrane. Previous studies revealed that polyacids can strongly interact with PANI via hydrogen bonding and electrostatic interactions [33–35]. The intimately entangled double-strand structure of PANI-polyacid leads to a reduced porosity of the membrane [64]. Besides, the top layer of PANI-PAMPSA was more hydrophilic than other membranes, which effectively prevented the dissolution and permeation of organic solvents into the bulk PANI matrix.

To determine the membrane stability in organic solvents, PANI membranes were soaked in the above five solvents for one week. The undoped PANI was unstable in all of the solvents, as all five solvents turned blue due to the dissolution of PANI, and the dry mass of the soaked membrane was reduced by 10–20%. The PANI-HCl membrane was more stable in methanol and acetone than the undoped PANI membrane, as there was only a slight colour change and the soaked membrane mass decreased by 5%, and it was stable in all other solvents. Both the PANI-PSSA and PANI-PAMPSA membranes were stable in all solvents as the solvents were colorless after the one week, and the dry mass of the soaked membrane remained constant (within an error range of 1%). Furthermore, the FT-IR spectra of the PANI-PSSA and PANI-PAMPSA membranes before and after soaking in the five solvents were analyzed (Fig. S3). The spectra show that the characteristic bands of both PANI and the polyacids did not shift after the membrane was soaked in solvent. These results indicate that the polyacid doped PANI membranes were able to retain their physical integrity in a wide range of solvents, and were therefore promising membranes for OSN.

3.3. Membrane permeance

Membrane permeance was evaluated using three solvents: methanol, isopropanol and acetone. These solvents were chosen as they had different solubility parameters and swelling effects as discussed in Section 3.2. The undoped PANI membrane was not evaluated because it was not stable in any of the solvents used. Additionally, the flux across the PANI-PAMPSA membranes was so low in acetone and thus

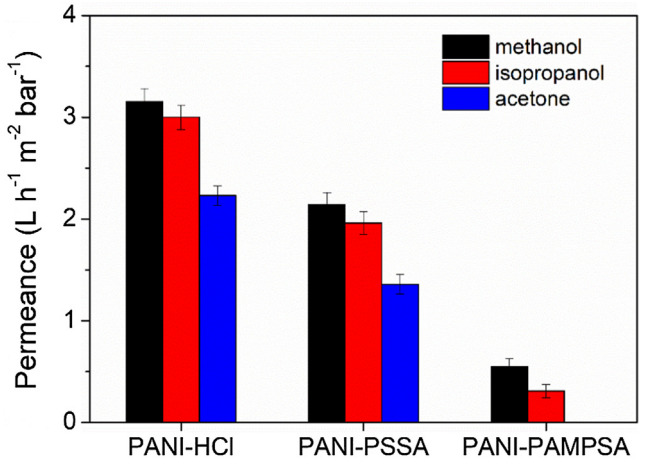

Fig. 8. Steady-state permeance of the doped PANI membranes in different solvents at 30 bar, 25 °C.

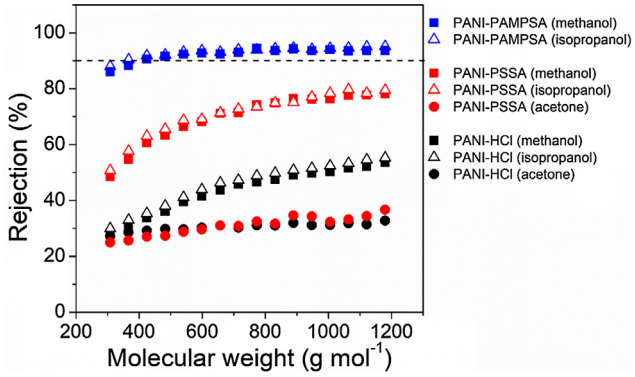

Fig. 9. MWCO curves of doped PANI membranes with PPG solution at 30 bar, 25 °C.

insufficient volume for determining the permeance and the MWCO.

The permeance of the doped PANI membranes experienced an initial drop due to the effect of membrane compaction under the transmembrane pressure [30,65]. The permeance became constant when an equilibrium was reached between the expansion effect of membrane swelling and the compaction effect of the applied pressure, which took approximately 30 min. Fig. 8 shows that the steady-state permeances of the doped PANI membranes were highly dependent on the dopant and the solvent used. In the same solvent, the permeance decreased with the increase of the dopant MW. In methanol, for example, PANI-HCl had the highest permeance (3.15 L h^{-1} m^{-2} bar^{-1}) followed by PANI-PSSA (2.14 L h^{-1} m^{-2} bar^{-1}) and PANI-PAMSPA (0.55 L h^{-1} m^{-2} bar^{-1}). Recalling the material properties and swelling profile, PANI-HCl had a larger free volume, thus leading to a higher permeance. In comparison, PANI-PAMPSA had a much lower permeance because it had a smaller free volume due to the doping of the PAMPSA macromolecules.

For the same type of membrane, the order of solvent from smallest to largest permeance was acetone < isopropanol < methanol. This order mirrored the already established swelling profile demonstrated in Fig. 7. This result suggests that the highest solvent permeance was generated by the solvent that swelled the membrane the most (methanol) and conversely, the lowest permeance was generated by the solvent that swelled the membrane the least (acetone). These results are in good consistence with previous studies that found swelling increased permeance as larger channels were formed in the polymer matrix [66,67].

3.4. Membrane MWCO

Fig. 9 shows that the three different doped PANI membranes generated distinct MWCO curves with the PPG rejections, which in general followed the order: PANI-HCl < PANI-PSSA < PANI-PAMPSA. The different PPG rejections were attributed to the different free volumes in the thin skin layers of the doped PANI membranes. The skin layer was dependent on the MW and interaction between PANI and the acid dopants. A higher swelling degree should yield a lower solute rejection because of the expansion of the polymer matrix by the solvent. This was directly reflected in the PPG rejections, where the most swollen PANI-HCl membrane had the lowest rejection and the least swollen PANI-PAMPSA had the highest rejection.

For PANI-PAMPSA, the MWCO curves in methanol and isopropanol were similar and the MWCO value was found to be around 400 g mol^{-1}. Therefore, PANI-PAMPSA can be classified as a NF membrane (*i.e.*, with a typical MWCO range of 200–1000 g mol^{-1}). To evaluate the stability of the PANI-PAMPSA membrane, three PANI-PAMPSA membrane samples were soaked in isopropanol for 1, 7, and 14 days, respectively, before the NF experiments. The MWCO curves of these membranes were highly identical with a MWCO range of 370–400 g mol^{-1} (Fig. S4). For PANI-PSSA, the MWCO curves in methanol and isopropanol were similar. The PPG rejections by PANI-PSSA were always below 90% throughout the MW range of 308 and 1179 g mol^{-1}, with the rejection of the 1179 g mol^{-1} PPG oligomer approximately 79%. This suggests that PANI-PSSA can be classified as a 'tight' ultrafiltration (UF) membrane (*i.e.*, with a typical MWCO range of 1000–10,000 g mol^{-1}). For PANI-HCl, the rejection of the 1179 g mol^{-1} PPG oligomer was 55%, which means that PANI-HCl was 'looser' than PANI-PSSA. The specific MWCO values of PANI-PSSA and PANI-HCl can be determined using solutes that are larger than the maximum MW of 1179 g mol^{-1} used in this work.

The PANI-HCl and PANI-PSSA membranes gave poor rejections in acetone, in comparison to those in methanol and isopropanol. The flat curves obtained indicate that there were probably defects inside the membranes, which could not discriminate between different PPG molecules. These membranes may need further treatment or alternative dopants for utilization in polar aprotic and nonpolar solvents.

4. Conclusions

This study systematically investigated the effect of polyacid dopants on the performance of PANI membranes in OSN. The PANI powder was synthesized by oxidative polymerization and the integrally skinned asymmetric PANI membranes was fabricated using immersion precipitation. The PANI membranes were then doped with HCl, PSSA and PAMPSA, respectively. FT-IR and XPS analysis confirmed the successful incorporation of acid dopants in the PANI polymer matrix. SEM images showed that large polyacids made the skin layer of the PANI membranes tight and smooth through interactions between PANI backbone and polyacids, without affecting the structure of the bulk support layer. Contact angle measurements revealed that the doped PANI membranes were more hydrophilic than the undoped PANI due to their hydrophilic acid groups. Stability tests showed that the polyacid doped PANI membranes had improved stability in a wide variety of organic solvents, and their swelling degrees decreased with the increase of the dopant MW. Preliminary NF experiments demonstrated that acid dopants played a key role in determining the permeance and separation performance of the membranes. The PANI-PAMPSA membrane had very high rejections in the NF range with an estimated MWCO of 400 g mol^{-1} in methanol and isopropanol. The PANI-HCl and PANI-PSSA membranes had UF characteristics. This study proved that polyacid doping is an important strategy to confer solvent stability and NF properties to PANI membranes. This simple approach can be broadly applied to designing new classes of OSN membranes for complicated chemical and refining processes in the future.

Acknowledgement

The authors acknowledge the financial support of the European Research Council (ERC) Consolidator grant TUNEMEM (Project reference: 646769; funded under H2020-EU.1.1.-EXCELLENT SCIENCE). The authors thank Dr. Lili Xu, Dr. Chris Davey and Dr. Agnieszka Holda (University of Bath) for useful discussion, National EPSRC XPS Users' Service (NEXUS) at Newcastle University for XPS analysis, and the technician team at the Department of Chemical Engineering, University of Bath for technical support. This manuscript is dedicated to Dr. Darrell Alec Patterson, BE(C&M) Hons, PostgradCert(ACADPRAC) Auck, DIC PhD Imperial, AIChemE (1974–2017).

Appendix A. Supplementary material

Supplementary data associated with this article can be found, in the online version, at https://doi.org/10.1016/j.seppur.2018.04.034.

References

[1] M. Priske, M. Lazar, C. Schnitzer, G. Baumgarten, Recent applications of organic solvent nanofiltration, Chem. Ing. Tech. 88 (2016) 39–49.
[2] P. Vandezande, L.E.M. Gevers, I.F.J. Vankelecom, Solvent resistant nanofiltration: separating on a molecular level, Chem. Soc. Rev. 37 (2008) 365–405.
[3] P. Marchetti, M.F. Jimenez Solomon, G. Szekely, A.G. Livingston, Molecular separation with organic solvent nanofiltration: A critical review, Chem. Rev. 114 (2014) 10735–10806.
[4] A.K. Hołda, I.F.J. Vankelecom, Understanding and guiding the phase inversion process for synthesis of solvent resistant nanofiltration membranes, J. Appl. Polym. Sci. 132 (2015) 1–17.
[5] A.R.D. Verliefde, E.R. Cornelissen, S.G.J. Heijman, E.M.V. Hoek, G.L. Amy, B.V.D. Bruggen, J.C. van Dijk, Influence of solute – membrane affinity on rejection of uncharged organic solutes by nanofiltration membranes, Environ. Sci. Technol. 43 (2009) 2400–2406.
[6] M.G. Buonomenna, J. Bae, Organic solvent nanofiltration in pharmaceutical industry, Sep. Purif. Rev. 44 (2015) 157–182.
[7] K. Werth, P. Kaupenjohann, M. Skiborowski, The potential of organic solvent nanofiltration processes for oleochemical industry, Sep. Purif. Technol. 182 (2017) 185–196.
[8] D.S. Sholl, R.P. Lively, Seven chemical separations to change the world, Nature 532 (2016) 435–438.
[9] B. Van der Bruggen, J. Geens, C. Vandecasteele, Influence of organic solvents on the performance of polymeric nanofiltration membranes, Sep. Sci. Technol. 37 (2002) 783–797.
[10] J.T. Scarpello, D. Nair, L.M. Freitas dos Santos, L.S. White, A.G. Livingston, The separation of homogeneous organometallic catalysts using solvent resistant nanofiltration, J. Membr. Sci. 203 (2002) 71–85.
[11] J. Pellegrino, The use of conducting polymers in membrane-based separations, Ann. N. Y. Acad. Sci. 984 (2003) 289–305.
[12] R. Mukherjee, R. Sharma, P. Saini, S. De, Nanostructured polyaniline incorporated ultrafiltration membrane for desalination of brackish water, Environ. Sci. Water Res. Technol. 1 (2015) 893–904.
[13] M.R. Anderson, B.R. Mattes, H. Reiss, R.B. Kaner, Conjugated polymer films for gas separations, Science 252 (1991) 1412–1415.
[14] G. Illing, K. Hellgardt, R.J. Wakeman, A. Jungbauer, Preparation and characterisation of polyaniline based membranes for gas separation, J. Membr. Sci. 184 (2001) 69–78.
[15] S. Kuwabata, C.R. Martin, Investigation of the gas-transport properties of polyaniline, J. Membr. Sci. 91 (1994) 1–12.
[16] G. Illing, K. Hellgardt, M. Schonert, R.J. Wakeman, A. Jungbauer, Towards ultrathin polyaniline films for gas separation, J. Membr. Sci. 253 (2005) 199–208.
[17] I.J. Ball, S.-C. Huang, K.J. Miller, R.A. Wolf, J.Y. Shimano, R.B. Kaner, The pervaporation of ethanol/water feeds with polyaniline membranes and blends, Synth. Met. 102 (1999) 1311–1312.
[18] I.J. Ball, S.-C. Huang, R.A. Wolf, J.Y. Shimano, R.B. Kaner, Pervaporation studies with polyaniline membranes and blends, J. Membr. Sci. 174 (2000) 161–176.
[19] M. Sairam, S.K. Nataraj, T.M. Aminabhavi, S. Roy, C.D. Madhusoodana, Polyaniline membranes for separation and purification of gases, liquids, and electrolyte solutions, Sep. Purif. Rev. 35 (2006) 249–283.
[20] L. Rebattet, M. Escoubes, M. Pinéri, E.M. Geniès, Gas sorption in polyaniline powders and gas permeation in polyaniline films, Synth. Met. 71 (1995) 2133–2137.
[21] D. Li, J. Huang, R.B. Kaner, Polyaniline nanofibers: A unique polymer nanostructure for versatile applications, Acc. Chem. Res. 42 (2009) 135–145.
[22] S. Zhu, M. Shi, S. Zhao, Z. Wang, J. Wang, S. Wang, Preparation and characterization of a polyethersulfone/polyaniline nanocomposite membrane for ultrafiltration and as a substrate for a gas separation membrane, RSC Adv. 5 (2015) 27211–27223.
[23] S. Zhao, Z. Wang, J. Wang, S. Wang, Poly(ether sulfone)/polyaniline nanocomposite membranes: Effect of nanofiber size on membrane morphology and properties, Ind. Eng. Chem. Res. 53 (2014) 11468–11477.
[24] S. Moulik, S. Nazia, B. Vani, S. Sridhar, Pervaporation separation of acetic acid/water mixtures through sodium alginate/polyaniline polyion complex membrane, Sep. Purif. Technol. 170 (2016) 30–39.
[25] R. Surya Murali, M. Padaki, T. Matsuura, M.S. Abdullah, A.F. Ismail, Polyaniline in situ modified halloysite nanotubes incorporated asymmetric mixed matrix membrane for gas separation, Sep. Purif. Technol. 132 (2014) 187–194.
[26] B. Hudaib, V. Gomes, J. Shi, C. Zhou, Z. Liu, Poly (vinylidene fluoride)/polyaniline/MWCNT nanocomposite ultrafiltration membrane for natural organic matter removal, Sep. Purif. Technol. 190 (2018) 143–155.
[27] M. Wan, J. Yang, Mechanism of proton doping in polyaniline, J. Appl. Polym. Sci. 55 (1995) 399–405.
[28] E.T. Kang, K.G. Neoh, K.L. Tan, Polyaniline: A polymer with many interesting intrinsic redox states, Prog. Polym. Sci. 23 (1998) 277–324.
[29] X.X. Loh, M. Sairam, A. Bismarck, J.H.G. Steinke, A.G. Livingston, K. Li, Crosslinked integrally skinned asymmetric polyaniline membranes for use in organic solvents, J. Membr. Sci. 326 (2009) 635–642.
[30] M. Sairam, X.X. Loh, K. Li, A. Bismarck, J.H.G. Steinke, A.G. Livingston, Nanoporous asymmetric polyaniline films for filtration of organic solvents, J. Membr. Sci. 330 (2009) 166–174.
[31] J. Shuping, M. Liu, S. Chen, Y. Chen, Complexation between poly(acrylic acid) and poly(vinylpyrrolidone): Influence of the molecular weight of poly(acrylic acid) and small molecule salt on the complexation, Eur. Polym. J. 41 (2005) 2406–2415.
[32] H. Hoffmann, K. Kamburova, H. Maeda, T. Radeva, Investigation of pH dependence of poly(acrylic acid) conformation by means of electric birefringence, Colloids Surf., A 354 (2010) 61–64.
[33] L. Sun, H. Liu, R. Clark, S.C. Yang, Double-strand polyaniline, Synth. Met. 84 (1997) 67–68.
[34] O.L. Gribkova, A.A. Nekrasov, M. Trchova, V.F. Ivanov, V.I. Sazikov, A.B. Razova, V.A. Tverskoy, A.V. Vannikov, Chemical synthesis of polyaniline in the presence of poly(amidosulfonic acids) with different rigidity of the polymer chain, Polymer 52 (2011) 2474–2484.
[35] J.-W. Jeon, Y. Ma, J.F. Mike, L. Shao, P.B. Balbuena, J.L. Lutkenhaus, Oxidatively stable polyaniline:polyacid electrodes for electrochemical energy storage, PCCP 15 (2013) 9654–9662.
[36] W.L. Jolly, Modern Inorganic Chemistry, McGraw-Hill, 1991.
[37] A.J. Heeger, Polyaniline with surfactant counterions: Conducting polymer materials which are processible in the conducting form, Synth. Met. 57 (1993) 3471–3482.
[38] G.R. Guillen, Y. Pan, M. Li, E.M.V. Hoek, Preparation and characterization of membranes formed by nonsolvent induced phase separation: A review, Ind. Eng. Chem. Res. 50 (2011) 3798–3817.
[39] P. Chapman, X.X. Loh, A.G. Livingston, K. Li, T.A.C. Oliveira, Polyaniline membranes for the dehydration of tetrahydrofuran by pervaporation, J. Membr. Sci. 309 (2008) 102–111.
[40] C. Reichardt, T. Welton, Solvents and Solvent Effects in Organic Chemistry, Fourth, Updated and Enlarged ed., Wiley, Germany, 2011.
[41] C.M. Hansen, Hansen Solubility Parameters: A User's Handbook, second ed., CRC Press, USA, 2007.
[42] A.F.M. Barton, Handbook of Solubility Parameters and Other Cohesion Parameters, CRC Press, USA, 1983.
[43] L.W. Shacklette, C.C. Han, Solubility and dispersion characteristics of polyaniline, MRS Proc. 328 (1993).
[44] R. Rohani, M. Hyland, D. Patterson, A refined one-filtration method for aqueous based nanofiltration and ultrafiltration membrane molecular weight cut-off determination using polyethylene glycols, J. Membr. Sci. 382 (2011) 278–290.
[45] C.J. Davey, Z.-X. Low, R.H. Wirawan, D.A. Patterson, Molecular weight cut-off determination of organic solvent nanofiltration membranes using poly(propylene glycol), J. Membr. Sci. 526 (2017) 221–228.
[46] J. Winter, B. Barbeau, P. Bérubé, Nanofiltration and tight ultrafiltration membranes for natural organic matter removal – Contribution of fouling and concentration polarization to filtration resistance, Membranes 7 (2017) 34.
[47] H. Kawashima, H. Goto, Preparation and properties of polyaniline in the presence of trehalose, Soft Nanosci. Lett. 01 (03) (2011) 5.
[48] J. Jang, J. Ha, J. Cho, Fabrication of water-dispersible polyaniline-poly(4-styrenesulfonate) nanoparticles for inkjet-printed chemical-sensor applications, Adv. Mater. 19 (2007) 1772–1775.
[49] V.V. Lyutov, S.D. Ivanov, V.M. Mirsky, V.T. Tsakova, Polyaniline doped with poly (acrylamidomethylpropanesulphonic acid): electrochemical behaviour and conductive properties in neutral solutions, Chem. Pap. 67 (2013) 1002–1011.
[50] S. Stan Corneliu, M. Popa, M. Olariu, S. Secula Marius, Synthesis and characterization of PSSA-polyaniline composite with an enhanced processability in thin films, Open Chem. 13 (2014).
[51] L. Hechavarría, H. Hu, M.E. Rincón, Polyaniline–poly(2-acrylamido-2-methyl-1-propanosulfonic acid) composite thin films: structure and properties, Thin Solid Films 441 (2003) 56–62.
[52] J.E. Tanner, Diffusion in a polymer matrix, Macromolecules 4 (1971) 748–750.
[53] S. Gam, J.S. Meth, S.G. Zane, C. Chi, B.A. Wood, M.E. Seitz, K.I. Winey, N. Clarke, R.J. Composto, Macromolecular diffusion in a crowded polymer nanocomposite, Macromolecules 44 (2011) 3494–3501.
[54] Y. Chen, E.T. Kang, K.G. Neoh, S.L. Lim, Z.H. Ma, K.L. Tan, Intrinsic redox states of polyaniline studied by high-resolution X-ray photoelectron spectroscopy, Colloid Polym. Sci. 279 (2001) 73–76.
[55] M.M. Mahat, D. Mawad, G.W. Nelson, S. Fearn, R.G. Palgrave, D.J. Payne, M.M. Stevens, Elucidating the deprotonation of polyaniline films by X-ray photoelectron spectroscopy, J. Mater. Chem. C 3 (2015) 7180–7186.
[56] T.A. Skotheim, J. Reynolds, Conjugated Polymers: Processing and Applications,

CRC Press, 2006.
[57] M. Canales, J. Torras, G. Fabregat, A. Meneguzzi, C. Alemán, Polyaniline emeraldine salt in the amorphous solid state: Polaron versus bipolaron, J. Phys. Chem. B 118 (2014) 11552–11562.
[58] C.A. Smolders, A.J. Reuvers, R.M. Boom, I.M. Wienk, Microstructures in phase-inversion membranes. Part 1. Formation of macrovoids, J. Membr. Sci. 73 (1992) 259–275.
[59] H. Deligöz, Preparation of self-standing polyaniline-based membranes: Doping effect on the selective ion separation and reverse osmosis properties, J. Appl. Polym. Sci. 105 (2007) 2640–2645.
[60] O.D. Iakobson, O.L. Gribkova, A.R. Tameev, V.V. Kravchenko, A.V. Egorov, A.V. Vannikov, Conductive composites of polyaniline–polyacid complex and graphene nanostacks, Synth. Met. 211 (2016) 89–98.
[61] W. Leng, S. Zhou, G. Gu, L. Wu, Wettability switching of SDS-doped polyaniline from hydrophobic to hydrophilic induced by alkaline/reduction reactions, J. Colloid Interface Sci. 369 (2012) 411–418.
[62] E.S. Tarleton, J.P. Robinson, S.J. Smith, J.J.W. Na, New experimental measurements of solvent induced swelling in nanofiltration membranes, J. Membr. Sci. 261 (2005) 129–135.
[63] A. Randová, L. Bartovská, Š. Hovorka, T. Bartovský, P. Izák, M. Kárászová, O. Vopička, V. Lindnerová, New approach for description of sorption and swelling phenomena in liquid + polymer membrane systems, Sep. Purif. Technol. 179 (2017) 475–485.
[64] H.-S. Moon, J.-K. Park, Structural effect of polymeric acid dopants on the characteristics of doped polyaniline composites: Effect of hydrogen bonding, J. Polym. Sci., Part A: Polym. Chem. 36 (1998) 1431–1439.
[65] I.F.J. Vankelecom, K. De Smet, L.E.M. Gevers, A. Livingston, D. Nair, S. Aerts, S. Kuypers, P.A. Jacobs, Physico-chemical interpretation of the SRNF transport mechanism for solvents through dense silicone membranes, J. Membr. Sci. 231 (2004) 99–108.
[66] M.F.J. Dijkstra, S. Bach, K. Ebert, A transport model for organophilic nanofiltration, J. Membr. Sci. 286 (2006) 60–68.
[67] L. Leitner, C. Harscoat-Schiavo, R. Kapel, C. Vallieres, Organic solvent nanofiltration with a Poly(dimethylsiloxane) membrane: Parameters affecting its sieving properties, J. Appl. Polym. Sci. 131 (2014) 1–10.